Iron-stabilized nanocrystalline ZrO_2 solid solutions: Synthesis by combustion and thermal stability

Felipe Legorreta Garcia [a], Valdirene Gonzaga de Resende [b], Eddy De Grave [b],
Alain Peigney [a], Antoine Barnabé [a], Christophe Laurent [a,*]

[a] Université de Toulouse, CIRIMAT, CNRS-UPS-INP, Université Paul-Sabatier, 31062 Toulouse cedex 9, France
[b] NUMAT, Department of Subatomic and Radiation Physics, University of Ghent, Proeftuinstraat 86, B-9000 Gent, Belgium

* Corresponding author. Tel.: +33 5 61 55 61 22; fax: +33 5 61 55 61 63.
  E-mail address: laurent@chimie.ups-tlse.fr (C. Laurent).

A B S T R A C T

The synthesis of Fe^{3+}-stabilized zirconia by the nitrate/urea combustion route was investigated. Using several characterization techniques, including X-ray diffraction, field-emission-gun scanning electron microscopy and notably Mössbauer spectroscopy, it was possible to determine the appropriate amount of urea that allows to obtain a totally stabilized $Zr_{0.9}Fe_{0.1}O_{1.95}$ solid solution. The nanocrystalline zirconia solid solution is mostly tetragonal, but the presence of the cubic phase could not be ruled out. An in-depth study of the thermal stability in air showed that the Fe^{3+} solubility in the stabilized solid solution starts to decrease at about 875 °C which results in the formation of hematite (possibly containing some Zr^{4+}) at the surface of the zirconia grains and further provokes the progressive transformation into the monoclinic zirconia phase.

Keywords:
A. Oxides
B. Chemical synthesis
C. Mössbauer spectroscopy
C. X-ray diffraction

1. Introduction

Zirconia (ZrO_2) is one of the materials of greater importance due to its excellent refractory properties, high chemical stability and mechanical resistance. At room temperature, pure zirconia is found as a monoclinic phase (henceforward indicated as m-ZrO_2). It exhibits structural transformations when increasing the temperature, transforming into tetragonal zirconia (t-ZrO_2) at approximately 1170 °C and cubic zirconia (c-ZrO_2) around 2370 °C [1]. The cubic form adopts the CaF_2 fluorine structure and has a simple cubic packing of the oxygen ions with the Zr^{4+} cations in half of the available sites with eightfold oxygen coordination. The tetragonal phase may be regarded as a slight distortion of one of the three axes of the cubic phase and by the shift of the oxygen ion from its ideal position in the fluorine structure. The Zr^{4+} cations are still coordinated by eight oxygen ions [1]. The monoclinic form contains Zr^{4+} cations in sevenfold oxygen coordination. The use of pure zirconia powders for sintering in order to produce dense materials or for applications that require high temperatures is limited due to the volumetric changes accompanying the reversible monoclinic-tetragonal phase transformations. It is well known that metal cations (notably Ca^{2+}, Mg^{2+}, Y^{3+} and some rare earth cations) form solid solutions with zirconia, thus stabilizing

either the tetragonal or cubic form, at increasing contents. The substitution of Zr^{4+} cations by lower valence cations is balanced by the formation of oxygen vacancies, which enhances the diffusion coefficient of the oxide anion and increases the ionic conductivity and therefore the performance of the material as a solid electrolyte. Stabilized zirconia has many mechanical, electronic, biomedical and chemical applications.

The influence of iron as a stabilizer was comparatively less studied. It was reported [2] that the addition of small amounts of hematite (α-Fe_2O_3) in stabilized ZrO_2 leads firstly to a significant increase in density during sintering without destabilizing the tetragonal phase and secondly to an increase of creep rates by a factor of 4–6. The incorporation of Fe^{3+} ions in the zirconia lattice was investigated using several preparation methods. Davison et al. [3] investigated the formation of solid solutions between α-Fe_2O_3 and ZrO_2 using the nitrate decomposition and calcination route. After calcination in air at 600 °C, they found a tetragonal solid solution for 2.5 and 5 at.% Fe^{3+} and a cubic solid solution for 10, 15 and 20 at.% Fe^{3+}. For higher iron contents, hematite is also detected. Berry et al. [4,5] used a similar route and showed that the incorporation of Fe^{3+} ions within t-ZrO_2 lattice at 500 °C stabilizes the cubic form and inhibits its transformation into the monoclinic form. A cubic solid solution containing as much as 50 at.% Fe^{3+} was obtained after calcination at 750 °C. The authors proposed from Mössbauer spectroscopy results that the stabilization of the cubic structure is associated with the presence of interstitial Fe^{3+} and oxygen vacancies. Calcination in air of the cubic solid solution at

1000 °C induces conversion to the monoclinic form (that may still contain a certain proportion of Fe^{3+} ions) and partial segregation of iron to form a hematite phase that probably contains some zirconium. Beck and Kaliba [6] prepared mixtures of α-Fe_2O_3 and ZrO_2 powders that were pressed in pellets and fired in air at 1500 °C. It is shown that 2 at.% of iron ions stabilize the tetragonal form and it is proposed that a considerable proportion of iron is in the divalent state due to the high temperature of firing. Li et al. [7] studied the influence of the size of the substituting trivalent cations in powders prepared by the precipitation–calcination route. Both undersized and oversized trivalent dopants are capable of stabilizing the tetragonal phase against monoclinic distortion, but the stability of tetragonal and cubic zirconia with undersized dopants is apparently lower than that with oversized dopants. Their main conclusions are as follows: (i) undersized dopants such as Fe^{3+} cause much larger distortion of the neighboring cation network than oversized dopants because of the asymmetric interatomic potential; (ii) the local environments of dopants in zirconia solid solutions are phase-insensitive and the characteristic oxygen polyhedron is MO_6 for undersized dopants and MO_8 for oversized dopants, with an M–O bond length very different from that of Zr–O; (iii) oxygen vacancies are associated with the Zr^{4+} cations in the case of oversized dopants, and with two dopant cations in the case of undersized dopants. This different availability of oxygen vacancies to Zr^{4+} cations is responsible for the different stabilization effects of oversized and undersized trivalent dopants. Inwang et al. [8] have studied the formation of solid solutions from the calcination of a xerogel. Depending on the pH of gel formation, either the tetragonal- or cubic-$Zr_{1-x}Fe_xO_{2-x/2}$ solid solution is obtained. A cubic phase with a high iron-doping ($Zr_{0.3}Fe_{0.7}O_{1.65}$) was obtained by calcination in air at 718 °C. However, the study suggests that the limiting iron solubility in the cubic phase decreases rapidly as the calcination temperature is raised, being about 20–30 at.% at 920 °C and below 2.5 at.% at 1200 °C. In calcined samples, a mixture of α-Fe_2O_3 and monoclinic solid solution is obtained. Popović et al. [9] have reported a maximum solubility of only 2 mol.% of α-Fe_2O_3 in m-ZrO_2 after a thermal treatment of the specimens at 1100 °C. They also proposed the possibility that for samples with 3 mol.% or more of α-Fe_2O_3, a small fraction of superparamagnetic α-Fe_2O_3 particles covers the surface of the zirconia particles. However, the authors were not able to further confirm their proposition. Štefanić et al. [10–12] prepared powders by calcination in air of amorphous precursors prepared by precipitation from aqueous solutions of iron and zirconium salts. An increase in the iron content tends to stabilize the cubic phase at the expense of the monoclinic phase. Mössbauer spectroscopy data indicate the presence of Fe^{3+} ions in both phases [10,12]. However, the solubility limit into zirconia decreases sharply upon the increase of the calcination temperature, which cause Fe^{3+} ions to segregate out of zirconia and form a α-Fe_2O_3 phase that is thought to contain some Zr^{4+} ions. Other researchers [13,14] have calcined gels at 600 °C in air. The method produces a mixture of m-ZrO_2 and t-ZrO_2, in the absence of iron, and it is shown that the incorporation of iron progressively favors the formation of the tetragonal solid solution, which is the sole phase obtained for 5 wt.% of iron. It is claimed that whereas no magnetically ordered iron oxide phase is detected, the Fe^{3+} ions are located in a monolayer at the external surface of the (1 1 1) planes of the zirconia particles [13] and that the surface of the particles is enriched in iron for low-loaded (<1–2 wt.% Fe) samples [14]. Other researchers investigating catalyst materials with low iron loadings have also reported that the Fe^{3+} ions have preference to be incorporated into the vacant surface sites of the ZrO_2 structure [15,16]. Using high-energy ball-milling of m-ZrO_2 and α-Fe_2O_3 powders for tens of hours, Jiang et al. [17] reported a stabilization into the cubic phase for an initial α-Fe_2O_3 content in the range 5–18.5 mol.%. The iron ions are in substitutional position and their increasing concentration causes a decrease in the cell parameter. During a subsequent heating in air, the cubic-to-tetragonal transition occurs at approximately 827 °C and the tetragonal-to-monoclinic transformation is absent below 950 °C. It occurs during cooling in the range 900–1100 °C. Both these transitions are accompanied by the formation of α-Fe_2O_3. However, a Mössbauer spectroscopy study reveals that Fe^{3+} ions are present in all three cubic, tetragonal and monoclinic phases. Ghigna et al. [18] prepared a c-$Zr_{0.9}Fe_{0.1}O_{1.9}$ solid solution by the so-called thermite reaction between metallic Zr and α-Fe_2O_3 and, in contrast to most other studies, it is claimed that iron enters the zirconia lattice mainly as Fe^{2+}, allocated in roughly equal amounts to two different distorted sites, one being substitutional and the other interstitial. Interestingly, it is shown that for the interstitial Fe^{2+}, the shorter iron–zirconium distance is only 0.364 nm and it is thus proposed that there is some direct iron–zirconium metallic bond, which is not usually known to occur in an oxide. These authors also report that iron oxides (FeO or α-Fe_2O_3) do not react with pure monoclinic zirconia under usual isothermal isobaric conditions. A study of the thermal stability in O_2 of such cubic solid solutions [19] suggested that the initially cubic phase may transform into the tetragonal form upon heating and that formation of m-ZrO_2 together with α-Fe_2O_3 occurs upon cooling from the calcination temperature. The formation of m-ZrO_2 and α-Fe_2O_3 is all the more pronounced when the calcination temperature is increased in the range 800–1050 °C. Bohé et al. [20] prepared a solid solution from ZrO_2 and Fe_2O_3 powders mixed in equal mass proportion and heated at 800 °C. These authors concluded that the incorporation of Fe^{3+} ions in the t-ZrO_2 structure stabilizes the cubic phase and inhibits its transformation to monoclinic phase. However, it is claimed that the tetragonal-to-monoclinic phase transformation upon annealing in air is enhanced. Kiminami [21] claimed that small additions (>1 mol.%) of hematite into the zirconia structure increase the hysteresis gap of the monoclinic-tetragonal transformation.

Thus, it appears that the preparation method has a strong influence on the degree of incorporation of iron ions, either di- or tri-valent and either as substitutional or interstitial ions, into the monoclinic, the tetragonal and the cubic zirconia lattices. In the present paper, it is proposed to use the nitrate-urea combustion route, which uses cheap reactants, produces gram-scale quantities of powders at the laboratory scale and can be readily upscaled. This method has proven very useful for the synthesis of various oxide solid solutions including $Mg_{1-x}M_xAl_2O_4$ (M = Fe, Co, Ni) [22–24], $Mg_{1-x}M_xO$ (M = Fe, Co) [25–27] and $Al_{1.8}Fe_{0.2}Al_3$ [28]. Ringuedé et al. [29] have used this method for the synthesis of mixtures of α-Fe_2O_3 and yttria-stabilized zirconia (25/75 and 50/50 volume fractions). We have investigated the influence of the urea content on the formation of the stabilized $Zr_{0.9}Fe_{0.1}O_{1.95}$ solid solution and its thermal stability in air. An exhaustive Mössbauer spectroscopy study was performed. The formation of Fe–ZrO_2 nanocomposite powders by selective reduction of the solid solution in hydrogen will be reported elsewhere [30].

2. Experimental methods

2.1. Powder synthesis by combustion

The appropriate amounts of $Fe(NO_3)_3 \cdot 9H_2O$ and $ZrO(NO_3)_2 \cdot xH_2O$ were dissolved in deionized water (20 mL, 70 °C) with varying amounts of urea, in order to produce 5 g of $Zr_{0.9}Fe_{0.1}O_{1.95}$ solid solution. The urea proportions were calculated by considering the total oxidizing valence (V_O) and reducing valence (V_R) of the different species [31,32]. The total oxidizing valence of the nitrates is $V_O = 10.5$. The reducing valence of urea is $V_R = 6$. The molar

quantity of urea (m) is first calculated so that the so-called stoichiometric ratio $\Phi_e = m \cdot V_R / V_O$ is equal to unity, which gives $m = 1.75$. However, as discussed by Zhang and Stangle [33], this method involves some approximations. Firstly, the oxidizing valence of the air in the atmosphere is not taken into account, which affects V_O. Secondly, the nitrogen-containing products are considered as being only N_2 (thus, zero is taken as the valence of nitrogen element) despite that nitrogen oxides and/or NH_3 can be formed in usually undetermined proportions. This affects both V_O and V_R. Hence it is necessary to experimentally determine the urea proportion suitable for a particular synthesis and thus the present syntheses were performed for ten different values of Φ_e (1–10), i.e. different values of m (1.75–17.5). However, for the sake of simplicity, we use the integer n ($n = 1, 2, 3, 4, 5, 6, 7, 8, 9$ and 10), which represents the multiplying factor rather than the molar quantity. The dish containing the solution was placed in a furnace pre-heated at 600 °C, keeping the door of the furnace open. After water evaporation, a combustion reaction takes place according to a redox reaction between the nitrates and urea, producing an oxide powder (henceforward named the as-prepared powder). The as-prepared powders will be designated as ZF-nU, with $n = 1, 2, 3, 4, 5, 6, 7, 8, 9$ and 10.

2.2. Thermal stability of the $Zr_{0.9}Fe_{0.1}O_{1.95}$ solid solution in air

A selected specimen (ZF-7U) was chosen to perform the study of the thermal stability in air. Batches of 80 mg of the $Zr_{0.9}Fe_{0.1}O_{1.95}$ powder were calcined in flowing air (4.8 L/h) at 625, 700, 725, 800, 825, 850, 875, 925, 975, 1000, 1025, 1175 and 1225 °C, yielding powders henceforward referred to as C625, …, C1125. A heating and cooling rate of 20 °C/min was applied (no dwell time at the target temperature).

2.3. Characterization

Powder X-ray diffraction (XRD) patterns for phase analysis and Rietveld refinements were obtained firstly at room temperature using a Bruker-AXS D4 Endeavor diffractometer (Cu (Kα_1, Kα_2), scan step increment = 0.02°, counting time = 5 s/step) and secondly for temperatures between 30 and 1200 °C using a Bruker-AXS D8 Advance diffractometer (Cu (Kα_1, Kα_2), scan step increment = 0.022°, counting time = 0.2 s/step). Spectra were collected every 100 °C from 30 to 600 °C and every 25 °C from 600 to 1200 °C. The Rietveld method implemented in the FullProf program [34] was used for crystal structure refinements. The proportions of tetragonal and monoclinic zirconia phases were evaluated from the XRD patterns using the Garvie-Nicholson method [35]. They were confirmed by the scale factor determined by the Rietveld refinement [36]. The XRD average crystallite size calculated for tetragonal zirconia corresponds to the spherical crystallite size calculated by the Scherrer formula using the full-width at half maximum (FWHM) of the tetragonal (1 0 1) Bragg peak corrected by the instrumental contribution.

The carbon content for the as-prepared powders was determined by flash combustion and is always lower than 0.2 wt.%, which is within the margin of error of the technique. Specific-surface-area measurements for the as-prepared and calcined powders were performed using N_2 adsorption at liquid N_2 temperature in a Micromeritics Flow Sorb II 2300 apparatus (BET method). This instrument gives a specific-surface-area value from one point (i.e. one adsorbate pressure) and requires calibration. The reproducibility of the results was determined to be in the ±3% range. The as-prepared powders, metallized with Pt, were observed by field-emission gun scanning electron microscopy (FEG-SEM JEOL JSM 6700F). Differential thermal analysis (DTA Netzsch 404S) on a selected powder was performed in flowing air up to 1300 °C with a heating and cooling rate of 20 °C/min.

^{57}Fe Mössbauer spectra (MS) of the powders were collected with powders kept at 80 K and/or at room temperature (RT), using a spectrometer operating at constant acceleration mode with triangular reference signal. ^{57}Co (Rh) source was used. Accumulation of the data was performed with a multi-scaling PC board with 1024 channels, and the measurements were run until a background of at least 10^6 counts per channel was reached. The spectrometer was regularly calibrated by collecting at RT the spectrum of a standard metallic iron foil or of standard α-Fe_2O_3 powder, and the isomer shifts are referenced with respect to α-Fe at RT. In addition, an Integral Low-Energy Electron Mössbauer Spectroscopy (ILEEMS) measurement at RT was performed for sample C925. ILEEMS is a variant of conventional transmission Mössbauer spectroscopy [37] by which the low-energy electrons are counted. These electrons, with energy of $\sim$10 eV, are produced by after-effects following the decay of the probe nuclei in the absorber. As a consequence of this low energy, only an extremely thin surface layer ($\sim$5 nm), of the material is probed.

3. Results and discussion

3.1. Combustion synthesis

The dish containing the nitrate/urea solution is introduced rapidly in the furnace pre-heated at 600 °C. Water evaporation is observed, accompanied by a lowering of the furnace temperature by about 40 °C. Then the combustion takes place according to a redox reaction between the nitrates and urea. Neither red fumes characteristic of NO_2 formation nor the characteristic smell of ammonia was detected for any synthesis. A moderate flame is observed for samples with $n = 1$–5. Note that for $n = 5$, the flame is much less intense and that the material becomes incandescent at the end of the combustion. For samples $n = 6$–10, there is simply an incandescence of the material and no flame. The measured temperature of the thermocouple located close to the reaction vessel varies accordingly (Fig. 1a), increasing up to about 750 °C upon the increase of n from 1 to 5, whereas it is close to the imposed temperature (600 °C) for $n = 6$–10. Note that the maximum temperature reached in the vessel is probably higher than that recorded for the furnace. Note also that these temperatures should be viewed as nothing more than a straightforward way to traduce the observations of "no flame", "strong flame", etc. The total time from dish introduction to end of reaction, when no incandescence can be detected anymore, is shown in Fig. 1b. There is a slow increase from 2 to 4 min for $n = 1$–5, then a jump between $n = 5$ ($t = 4$ min) and $n = 6$ ($t = 6$ min), followed by a moderate increase up to 7.5 min for $n = 10$. This time increase reflects the increase of the water evaporation duration due to a more sluggish solution when the urea content is increased and also the fact that the process is slower when there is no flame (i.e. for $n = 6$–10).

It was verified that the as-prepared powders contain only trace amounts of carbon (less than 0.2 wt.%). Regarding the BET specific surface area (S_w), the specimens can again be separated into two groups. S_w is in the range 1.9–6 m^2/g for $n = 1$–5. For $n = 6$–10, S_w is significantly higher. It increases for $n = 6, 7, 8$ and 9 (30.3, 39.1, 39.3 and 45.2 m^2/g, respectively) and sharply decrease (28.3 m^2/g) for $n = 10$. The higher S_w for the second group of powders could reflect a smaller grain size, due to both the lower temperature reached during the combustion and the increasing expansion of the powder due to the higher release of gases for higher urea contents.

The XRD patterns of the as-prepared powders are shown in Fig. 2. It is possible to distinguish two groups of powders ($n = 1$–4 and $n = 5$–9) that are almost the same as the former ones (powder ZF-5U now falls in the second group), and an isolated powder, ZF-10U. For the first group ($n = 1$–4), monoclinic zirconia is detected
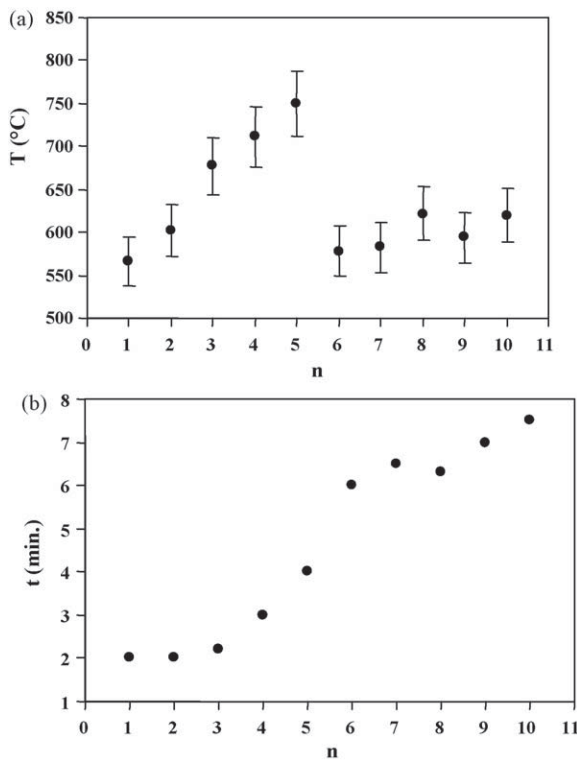
Fig. 1. Temperature reached by the furnace during combustion in a furnace pre-heated at 600 °C (a), time for completion of reaction (b) versus the proportion of urea (n) used for the combustion synthesis.
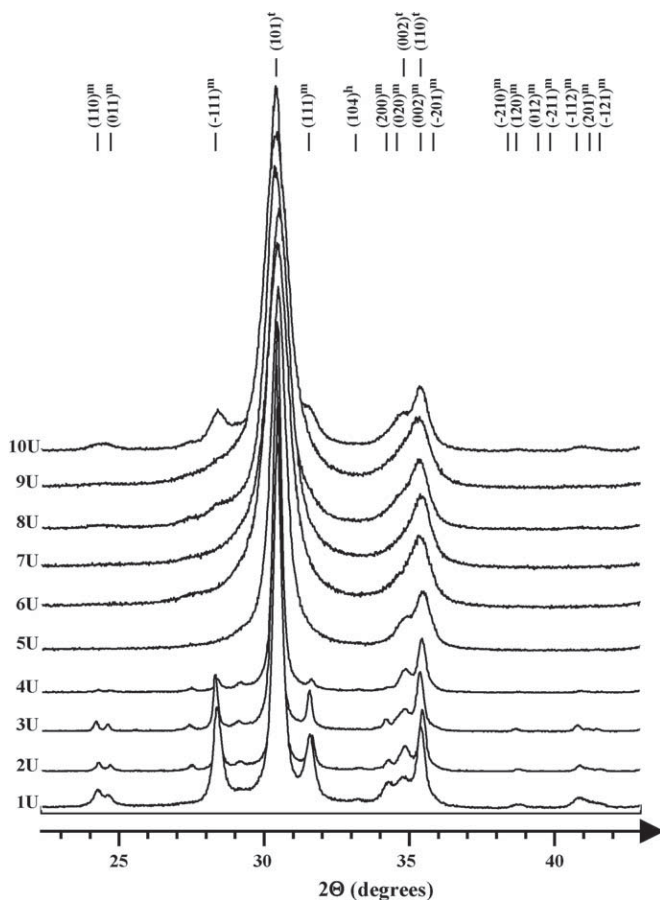

Fig. 2. XRD patterns of the as-prepared powders. The proportion of urea used for the combustion is indicated as 1U, 2U, ..., 10U.

Table 1

Cell parameters (a, c) for a tetragonal phase as deduced from Rietveld refinement of XRD patterns. a^* is equal to $a\sqrt{2}$ as in the fluorine cell. t-proportion (%) is the proportion of tetragonal phase evaluated from the XRD patterns (balance is monoclinic zirconia).

n	a (nm)	c (nm)	c/a^*	t-proportion (%)
1	0.35785(7)	0.5159(2)	1.019	76
2	0.35991(3)	0.51664(5)	1.019	88
3	0.35885(4)	0.51607(8)	1.017	89
4	0.35859(5)	0.51647(8)	1.018	96
5	0.35884(7)	0.5159(2)	1.017	100
6	0.35810(9)	0.5146(4)	1.016	98
7	0.3586(2)	0.5137(8)	1.013	100
8	0.35886(3)	0.5154(2)	1.016	97
9	0.3594(3)	0.5154(7)	1.014	100
10	0.35821(8)	0.5173(2)	1.021	90

(albeit with a lower proportion for powder ZF-4U) along with tetragonal zirconia, which is the major phase. The presence of the cubic form can neither be confirmed nor ruled out since there is no significant improvement of the reliability factors in the Rietveld analysis if this phase is included or not. The (1 0 4) peak of hematite (labelled (1 0 4)^h in Fig. 2) is faintly detected for ZF-1U and ZF-2U. For the second group (n = 5–9), hematite is not detected and only a very weak shoulder on the low 2θ-side of the (1 1 1) tetragonal peak could account for monoclinic zirconia for some powders. All diffraction peaks account for tetragonal zirconia. For ZF-10U, the monoclinic phase, but not hematite, is clearly detected in addition to the tetragonal phase. The proportion of the tetragonal phase with respect to all zirconia phases as calculated by the Garvie–Nicholson method [35] from the XRD patterns is indicated in Table 1. Rietveld refinement of the patterns gave the values of the (a, c) cell parameters of the tetragonal zirconia phase (Table 1). The values, which differ slightly from one powder to another, are by and large similar to those reported by other researchers for a tetragonal solid solution with 2.5 and 5 at.% [3] or 6 at.% [12] of iron. It is thus difficult to find a correlation between the parameters and the iron proportion actually incorporated in this phase for the present powders. One can note that these values are average values and need to be considered with the pure mathematical accuracy and with the refinement process accuracy. Considering the others parameters and results, the c/a differences between ZF-6U, ZF-7U, ZF-8U and ZF-9U do not seem to be significant. It is further noticed that the diffraction peaks of the tetragonal phase are markedly wider for the second group of powders (n = 5–9) and for ZF-10U than for the first group (n = 1–4).

Low-magnification FEG-SEM images (not shown) of the as-prepared powders reveal large grains, measuring tens of micrometers across, as well as micro- or submicrometric grains. The proportion of the latter ones tends to increase upon the increase of the urea proportion (n) due to the higher expansion occurring during the combustion reaction. Furthermore, the zirconia grains are quite porous, reflecting the escaping of gases during the combustion. The measurement of the dimension of the size of the primary grains (which may be monocrystalline) on high-magnification FEG-SEM images for ZF-1U (Fig. 3a), ZF-3U (Fig. 3b) and ZF-4U (Fig. 3c) reveal a decrease in the average size (85, 80 and 55 nm, respectively) as well as a narrowing of the size distribution. For ZF-7U (Fig. 3d) and ZF-9U (Fig. 3e), only very small clusters, smaller than about 10 nm, are observed on the surface. They either are zirconia crystallites or come from the Pt metallization, which in both cases indicates that the crystallite size and roughness are very low. For ZF-10U (Fig. 3f), the average primary grain/crystallite size is evaluated to be below about 30 nm. These data were compared to the XRD average crystallite size calculated by applying the Scherrer formula on the tetragonal (1 0 1) Bragg peak (Fig. 4). The
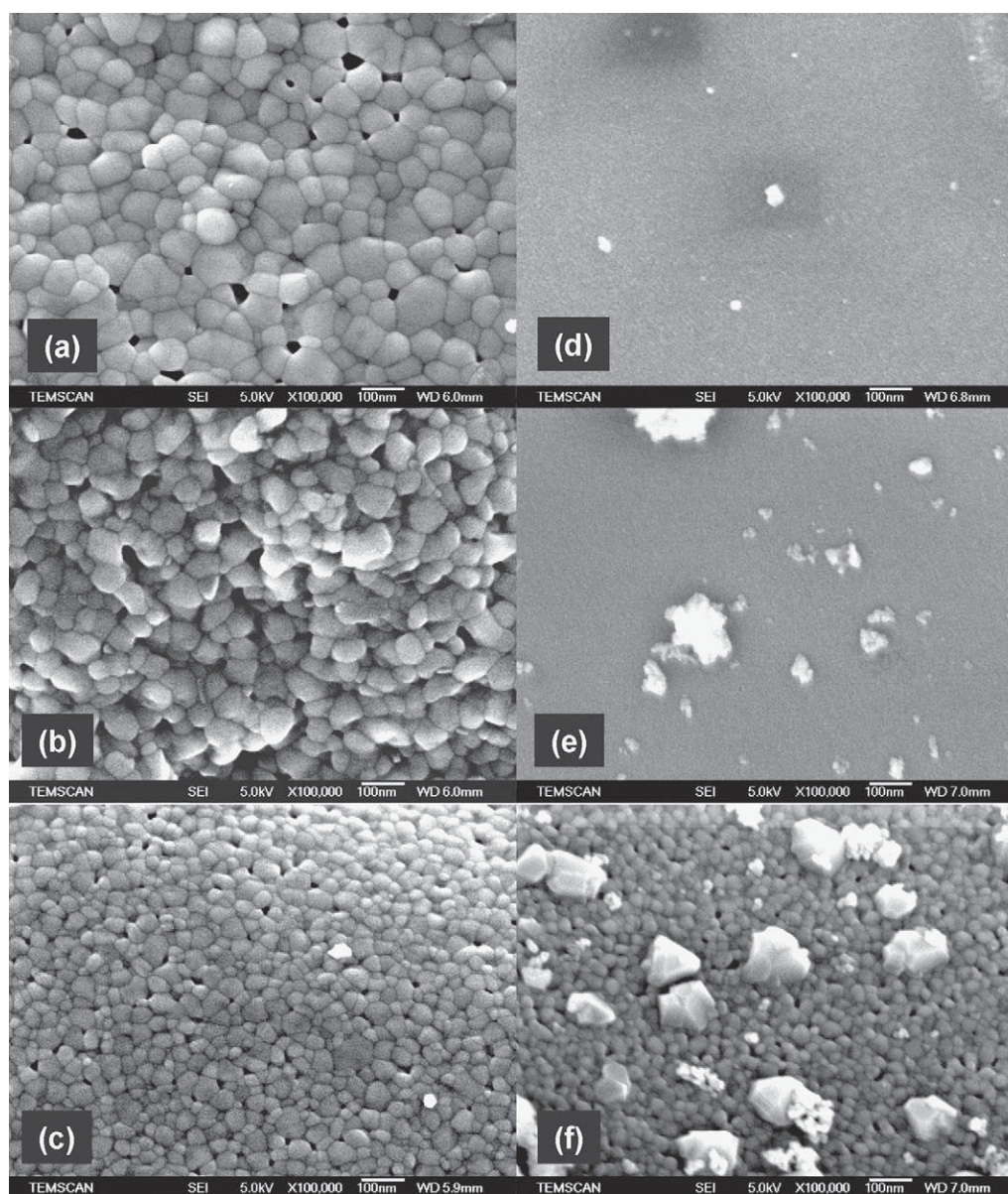
Fig. 3. FEG-SEM images of some as-prepared powders synthesized with different urea proportions (n): (a) $n = 1$; (b) $n = 3$; (c) $n = 4$; (d) $n = 7$; (e) $n = 9$; (f) $n = 10$.
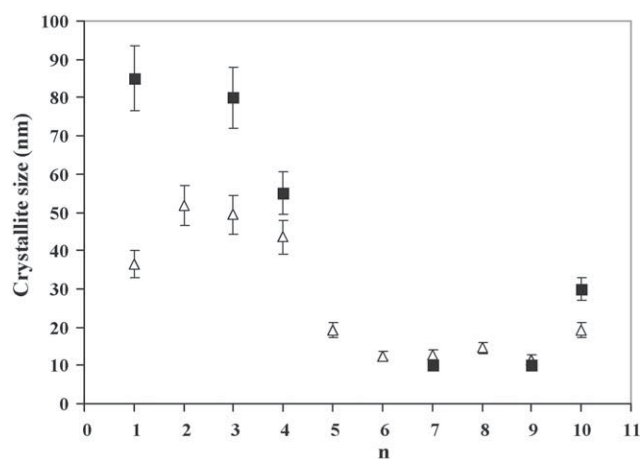

Fig. 4. Average crystallite size determined from the XRD pattern using the FWHM of the tetragonal (1 0 1) Bragg peak corrected by the instrumental contribution (squares) and from direct measurement on FEG-SEM images (triangles) versus the proportion of urea (n) used for the combustion synthesis.

agreement on the evolution and on the size for $n = 4$–10 are very good. The differences for $n = 1$–3 are due to the differences in the methods for size calculation. One can note that the size evolution is also in good agreement with the S_w results. No attempt was made to calculate a size based on the S_w results because the hypothesis of non-agglomerated particles is not verified in the present powders. Furthermore, it is noteworthy that the small crystalllite size measured for powders prepared with $n = 5$–9 are consistent with the above observation that all diffraction peaks for these materials account for tetragonal zirconia.

Mössbauer spectra (MS) of the as-prepared powders were computer-analyzed in terms of model-independent distributions of hyperfine-parameter values and numerical data quoted hereafter refer to maximum-probability values. MS collected at RT and 80 K for four powders of the first group ($n = 1, 3, 4$ and 5) (Fig. 5) are composed of a dominant doublet and one or two weak sextets. The adjusted parameter values are listed in Table 2. On the basis of the isomer shift ($\sim$0.35 mm/s at RT), the doublet can be attributed to Fe^{3+} in an O_6 co-ordination and, referring to the findings reported by other authors [4,5,11,17], it is reasonable to assume that it
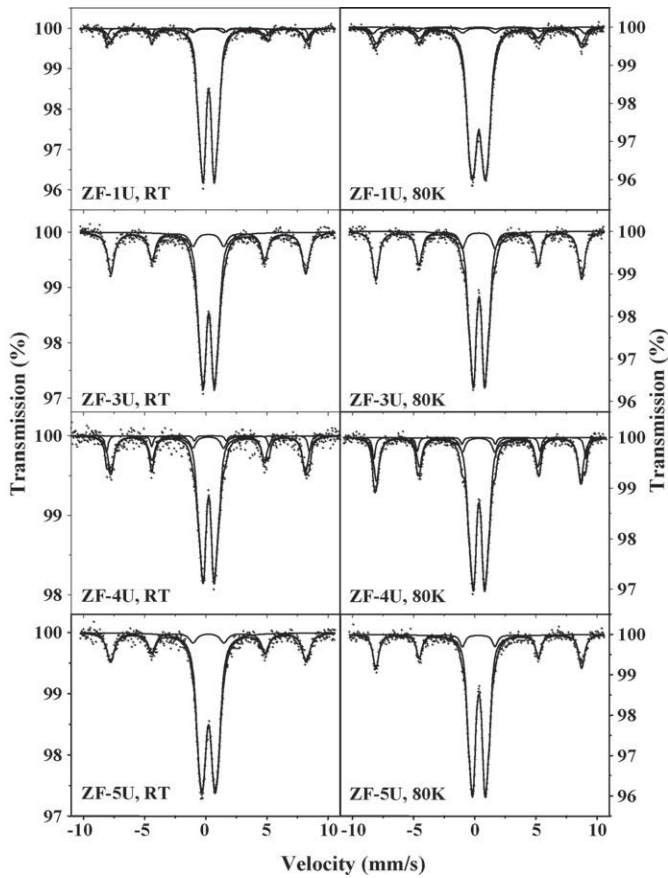
Fig. 5. Mössbauer spectra of the as-prepared powders prepared with a proportion of urea n = 1, 3, 4 or 5 collected at RT (left), 80 K (right).

concerns a tetragonal or cubic zirconia phase. This implies that there is no (or extremely few) iron present in a monoclinic zirconia phase. This conclusion is to some extent supported by observations [9,12] of a doublet with an isomer shift of ~0.40 mm/s at RT for Fe^{3+} in monoclinic zirconia. Such a doublet is not detected for the present powders.

Considering the hyperfine parameters of the outer sextet, resolved for two of the four samples (ZF-1U and ZF-4U), it is plausible to ascribe this component to hematite (α-Fe_2O_3). The sextet component present in the MS of all four samples of the first group was fitted with a hyperfine field H_{hf} distribution ranging between 490 and 505 kOe, keeping the quadrupole shift equal to zero. The maximum of the H_{hf} distribution was found to be ~493 kOe at RT and the isomer shift ~0.32 mm/s. Considering these

values and taking into account that all four powders exhibit a weak magnetism, as noticed using a hand magnet, it is tempting to suggest that the iron phase that is responsible for the sextet is maghemite (γ-Fe_2O_3). In spite of the existence of ferric ions in two different crystallographic environments, i.e., fourfold and sixfold oxygen co-ordinations, the Mössbauer spectrum of maghemite shows only one broad sextet because the hyperfine parameters of the two iron sites are similar in magnitude. In such case, using a model-independent hyperfine-field distribution to fit the spectrum is a proper approach [38]. It is not unreasonable that the presence of a γ-Fe_2O_3 phase has remained unnoticed from the XRD patterns since its main diffraction peaks are masked by the peaks of other species.

The MS collected at RT (Fig. 6, left pane) for the second group of samples (n = 6–10) consist of a broad quadrupole doublet that could be adequately reproduced in terms of model-independent quadrupole-splitting distributions (QSDs). It should be noted that the MS for powder ZF-10U is totally similar to the other MS although XRD data showed that this powder contains a fair amount of monoclinic zirconia. This observation confirms that the monoclinic phase contains no iron, as already suggested by the results for the first group of samples as discussed above. The evaluated QSD profiles are plotted on the right side of Fig. 6. The adjusted values of some relevant Mössbauer parameters (Table 3) are similar for all specimens. The QSD profiles are clearly multimodal, consistently showing four more or less well-resolved maxima. To quantify the profiles, superimpositions of four Gaussian curves were fitted to the evaluated QSD profiles. Each of these Gaussians is characterized by the position of its maximum, $\Delta E_{Q,m,i}$ (i = 1, 2, 3, 4) and by its relative area RA_i. The adjusted values for these parameters are presented in Table 4. Again, no obvious correlation of these values with the urea content used for the powder synthesis is apparent. It is believed that the occurrence of distinct maxima in the QSD profiles is real, thus suggesting different structural environments for the Fe^{3+} cations. However, one may show doubts regarding the significance of the fourth, high-ΔE_Q component centered at ~1.9 mm/s. This value is indeed extremely high for a ferric state, and more typical for a ferrous one, but on the other hand the isomer shift is too low for Fe^{2+}. It should be stressed though that the contribution of the high-ΔE_Q component is merely ~8% and consequently its hyperfine parameters are ill-defined in the strongly overlapping absorption envelope. Štefanić et al. [12] have reported that the doublet MS accounting for Fe^{3+} ions in tetragonal zirconia show two strongly overlapping quadrupole-split components, which could indicate the presence of two nonequivalent distributions of iron in the solid solution. Therefore, it is tempting to suggest that the present powders are composed of a mixture of tetragonal and cubic zirconia phases with the RT MS consisting of three contributions,

Table 2

Mössbauer parameters at RT and 80 K for the as-prepared powders prepared with a proportion of urea n = 1, 3, 4 or 5. H_{hf}: hyperfine field; $2\varepsilon_Q$: quadrupole shift; ΔE_Q: quadrupole splitting; δ: isomer shift; RA: relative spectral area; and *: fixed parameter.

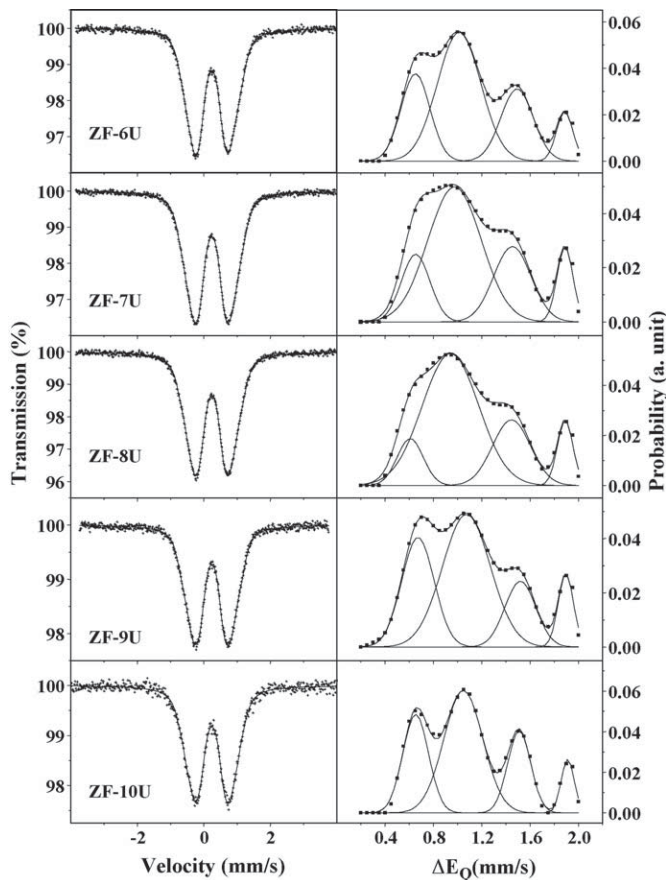| Powder	Hematite sextet				Maghemite sextet				Fe^{3+} doublet		
	H_{hf} (kOe)	$2\varepsilon_Q$ (mm/s)	RA (%)	δ (mm/s)	H_{hf} (kOe)	$2\varepsilon_Q$ (mm/s)	RA (%)	δ (mm/s)	ΔE_Q (mm/s)	RA (%)	δ (mm/s)
RT											
ZF-1U	514	−0.19	7	0.39	493	0.0 *	14	0.33	0.82	79	0.35
ZF-3U	–	–	–	–	493	0.0*	37	0.32	0.83	63	0.35
ZF-4U	514	-0.20*	8	0.39	493	0.0*	32	0.31	0.77	60	0.35
ZF-5U	–	–	–	–	493	0.0*	28	0.33	0.95	72	0.34
80 K											
ZF-1U	537*	−0.03	6	0.47	519	0.0*	17	0.46	1.09	77	0.45
ZF-3U	–	–	–	–	518	0.0*	40	0.44	0.84	60	0.47
ZF-4U	537	0.09	9	0.48	518	0.0*	32	0.43	0.82	59	0.46
ZF-5U	–	–	–	–	518	0.0*	29	0.44	0.96	71	0.45

Fig. 6. Mössbauer spectra of the as-prepared powders prepared with a proportion of urea $n = 6-10$ collected at RT (left), the corresponding QSD profiles (right).

Powder	$\Delta E_{Q,m,1}$	RA_1	$\Delta E_{Q,m,2}$	RA_2	$\Delta E_{Q,m,3}$	RA_3	$\Delta E_{Q,m,4}$	RA_4
ZF-6U	0.65	22	1.01	50	1.49	20	1.9	8
ZF-7U	0.65	14	0.98	56	1.45	21	1.9	9
ZF-8U	0.61	10	0.94	62	1.45	20	1.9	8
ZF-9U	0.67	27	1.07	49	1.52	16	1.9	8
ZF-10U	0.70	26	1.09	54	1.50	10	1.9	10

values of n ($n = 6-9$) a transition in the formation mechanisms seems to take place since the reaction temperature is observed to be much lower, while zirconia is nevertheless obtained as the sole stabilized phase and no free iron oxide is detected. Hence, no obvious parameter emerges that provides an indication as to why the urea proportions $n = 6-9$ yield the desired result, i.e. the stabilized $Zr_{0.9}Fe_{0.1}O_{1.95}$ solid solution. It is possible that the crystallite size of the zirconia species plays an important role in that respect as larger crystallites will more easily end up in the form of the stable monoclinic form. Increasing the urea proportion favors the emission of gases and therefore the expansion of the solid phase, which favors the formation of smaller crystallites. This mechanism could explain why no monoclinic zirconia is detected for $n = 6-9$ even though the reaction temperature is lower than for $n = 1-5$, for which an increase in reaction temperature obviously facilitates the formation of the tetragonal phase. The corresponding urea quantities ($n = 6-9$) could also favor the formation of suitable gel-like species by complexation of the Zr^{4+} and Fe^{3+} ions with urea, which could in turn trigger the direct incorporation of Fe^{3+} ions in the zirconia phase and therefore favor crystallization in stabilized form at moderate temperature. Further studies, notably on all intermediate species, would be required to totally elucidate the involved mechanisms. The powder ZF-7U, which is considered to be the desired $Zr_{0.9}Fe_{0.1}O_{1.95}$ solid solution in totally stabilized form, was selected to examine the thermal stability in air, the results of which are presented in the next section.

3.2. Thermal stability of the $Zr_{0.9}Fe_{0.1}O_{1.95}$ solid solution in air

The DTA curve (not shown) revealed weak endothermic peaks at about 650, 900 and 1150 °C (the latter extremely weak) during heating and a sharp exothermic peak at about 700 °C. Kiminami [21] reported weak and broad peaks during heating, indicating a low transformation rate, for a powder with 1 mol.% α-Fe_2O_3 and no observable peaks for 10 mol.%. From the analysis of the XRD patterns presented below, the peak at 900 °C is assigned to the transformation from the iron-stabilized solid solution to the mixture of m-ZrO_2 and α-Fe_2O_3. Comparing the present results to those reported for the DTA study of a $Zr_{0.9}Co_{0.1}O_{1.9}$ solid solution [39], it is proposed that the DTA peaks at 1150 °C (heating) and 700 °C (cooling) therefore respectively represent the monoclinic-to-tetragonal (heating) and tetragonal-to-monoclinic (cooling) transformations of ZrO_2.

XRD patterns were recorded at different temperatures between 30 and 1200 °C (Fig. 7). Up to 875 °C, only peaks of the tetragonal solid solution are detected. They are progressively more narrow, indicating crystallite growth. From 900 °C up to 1175 °C, peaks of both α-Fe_2O_3 and monoclinic zirconia are detected, both with increasing intensity, whereas the intensities of the tetragonal-phase peaks diminish. At 1175 and 1200 °C (Fig. 7c), it is observed that the proportion of t-ZrO_2 increases at the expense of that of m-ZrO_2, which reflects the expected transition that is known to occur at about 1170 °C at equilibrium. In order to prepare some specimens for the S_w and MS studies, batches of the as-prepared ZF-7U powder were calcined in air at different temperatures (625, 700, 725, 800, 825, 850, 875, 925, 975, 1000, 1025, 1175 and
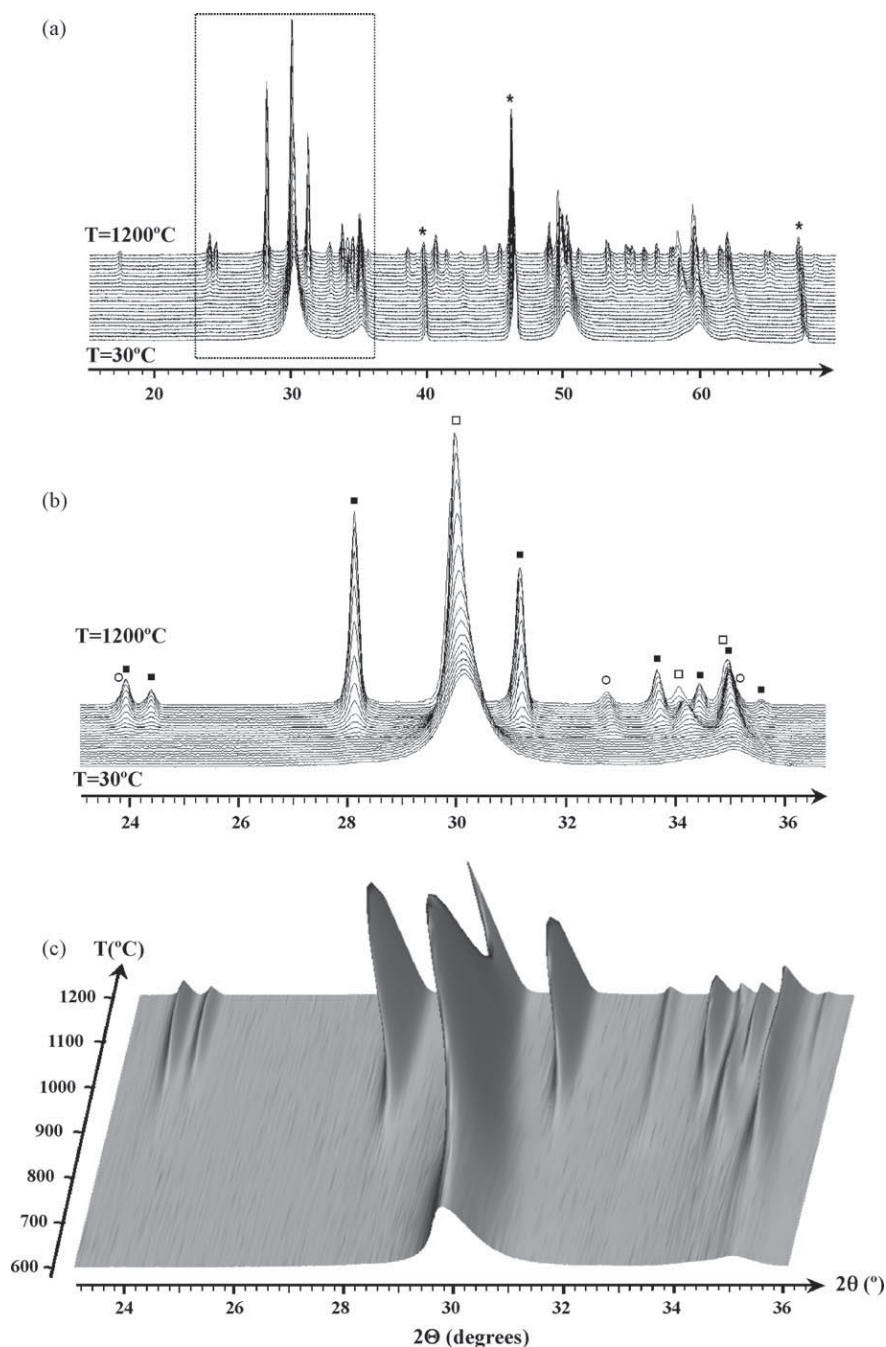
i.e. two (represented by $\Delta E_{Q,m,1}$ and $\Delta E_{Q,m,2}$) from different environments of the Fe^{3+} cations in the tetragonal phase and one (represented by $\Delta E_{Q,m,3}$) from the Fe^{3+} cations in the cubic phase, thus explaining the multi-modal appearance of the QSD profiles evaluated from the MS. Other researchers [5,17] have also reported that the quadrupole splitting is larger for the cubic phase than for the tetragonal phase. However, this suggestion seems speculative and more sound evidence from complimentary experiments is needed to strengthen any conclusion in that respect. Nevertheless, the evolution of the proportions ($RA_1 + RA_2$) and RA_3 versus n (Table 4) could indicate that the proportion of Fe^{3+} in the cubic phase (RA_3) tends to decrease for $n > 7-8$.

Increasing the urea proportion from $n = 1$ up to $n = 4$ increases both the reaction temperature and the proportion of tetragonal phase, but causes a lowering of the amount of iron incorporated in the latter phase. Further increasing the urea proportion up to $n = 5$ results in an increase of all three parameters. All zirconia is now stabilized in tetragonal form, but there still remains a certain proportion of iron present as a free iron oxide, probably in the form of finely dispersed maghemite particles. Subsequently, for higher

Powder	$\Delta E_{Q,m}$ (mm/s)	δ (mm/s)	Γ (mm/s)
ZF-6U	1.01	0.36	0.32
ZF-7U	0.93	0.35	0.33
ZF-8U	0.92	0.35	0.33
ZF-9U	1.07	0.35	0.30
ZF-10U	1.06	0.35	0.33

Fig. 7. (a) XRD patterns of powder ZF-7U recorded at different temperatures. Star marks indicate the Bragg peaks of the platinum crucible used; (b) detail of the 23.5–36.5° 2θ range. Phases are indexed as follows: t-ZrO$_2$ phase (open square), m-ZrO$_2$ (solid square), α-Fe$_2$O$_3$ (open circle); (c) three-dimensional view of the 23.5–36.5° 2θ range showing the increase of the tetragonal peak at high temperature.

1225 °C). It should be noted that the calcination conditions were similar to those applied for the DTA study, but quite different from those used for the aforementioned variable-temperature XRD study (see Experimental section). Nevertheless, the RT XRD patterns (not shown) for the powders calcined at a given temperature are similar to those recorded in situ at the corresponding temperatures. The evolution of the proportion of the tetragonal phase versus the calcination temperature (Fig. 8) shows that the transformation from the iron-stabilized solid solution to the mixture of m-ZrO$_2$ and α-Fe$_2$O$_3$ takes place between 875 and 1000 °C.

As could be expected, the specific surface areas of the powders (Fig. 8) decrease with increasing calcination temperature (ca. 40,

16, 9, 3.5, 2.5 and 2 m^2/g for the as-prepared (reported as C600), C625, C725, C825, C925 and C1025 powders, respectively). This variation reflects the crystallite growth, as detected by XRD, prior to the formation of hematite and to the simultaneous transformation of the zirconia phase.

The MS collected at RT and at 80 K for the powders calcined in air at different temperatures are shown in Figs. 9 and 10. They were computer-analyzed in terms of model-independent distributions of hyperfine-parameter values and numerical data quoted hereafter refer to maximum-probability values. The adjusted values of some relevant Mössbauer parameters are listed in Table 5. The MS of the C625 and C850 powders are composed of a single doublet that can be attributed to Fe^{3+}, most likely in O$_6$ coordination in the
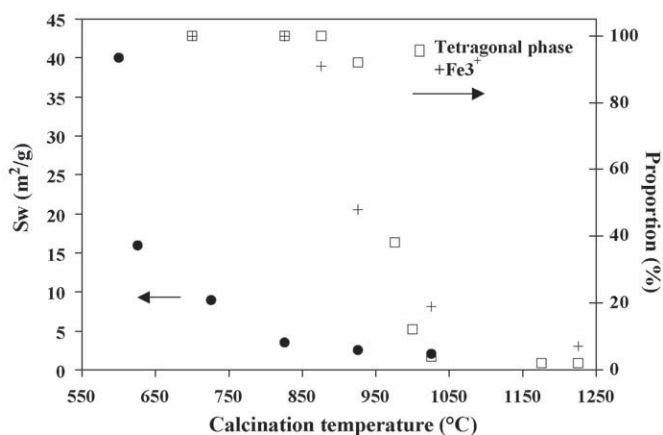
Fig. 8. Specific surface area of the powders calcined in air (solid circles), proportion of tetragonal zirconia (balance is monoclinic zirconia) evaluated from the XRD patterns (open squares), proportion of Fe^{3+} ions in tetragonal-zirconia solid solution calculated from ther Mössbauer spectra (+) versus the calcination temperature.

tetragonal phase. The MS of C875 (RT and 80 K) show a weak sextet ($\sim$9%), with hyperfine parameters characteristic of α-Fe_2O_3 in addition to the doublet. The XRD pattern for this sample did not show any indication of α-Fe_2O_3, probably because of the small amount of this phase. The MS of C925, C1025 and C1225 are composed of a doublet that weakens as the calcination temperature increases (the MS parameters of which are ill-defined and not reliable for C1225) and a dominant sextet (52, 81 and 93%, respectively), revealing the presence of an increasing amount of hematite, in agreement with the XRD results. The decrease of the doublet accounting for Fe^{3+} substituting in the tetragonal phase is
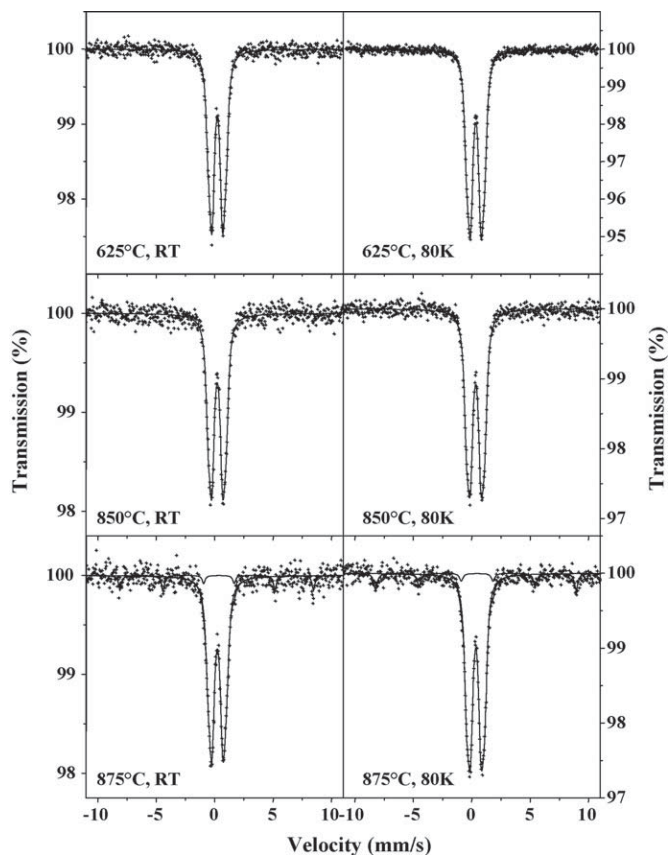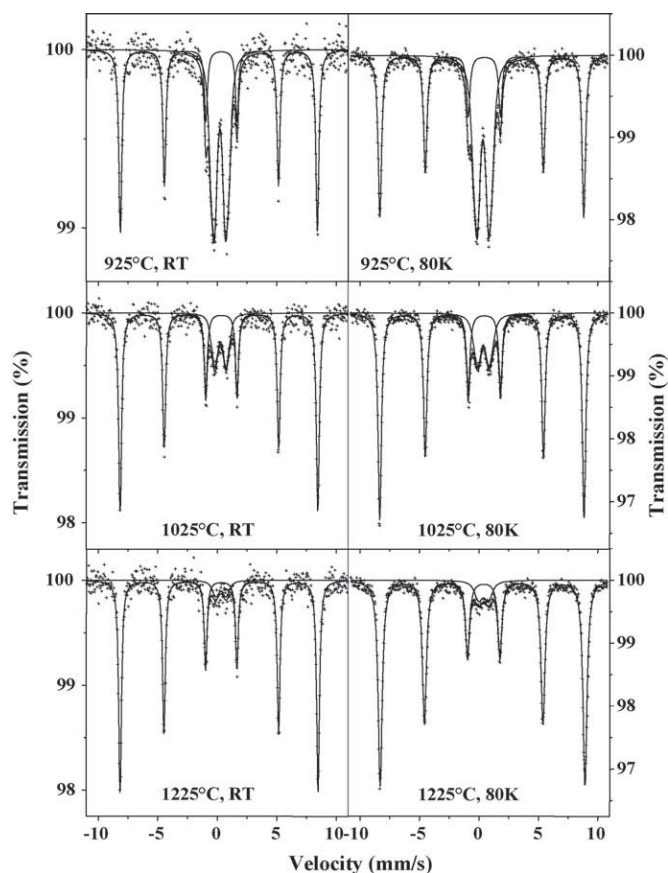
Fig. 10. Mössbauer spectra collected at RT (left), 80 K (right) of powder ZF-7U calcined in air at 925, 1025, and 1225 °C.

in line with the decrease of the proportion of this phase as deduced from the XRD patterns (Fig. 8). Considering the values of the quadrupole shift ($2\varepsilon_Q$) of the sextet, it may be concluded that the formed hematite possesses the weakly ferromagnetic spin state at 80 K. The finding that no Morin transition could be observed down to 80 K implies that small particles ($\sim$20 nm) are involved, or that a (slight) Zr^{4+}-for-Fe^{3+} substitution has taken place in the hematite structure Other researchers [9,12] have indeed reported that the calcination of Fe_2O_3–ZrO_2 solid solutions at 800 °C produces Zr^{4+}-substituted hematite, with a hyperfine field value lower than that for pure α-Fe_2O_3 (516 kOe). It is noted for the present powders that the lower the calcination temperature, the lower is the hyperfine field. Indeed, a slight decrease from 516 kOe for C1225 to 513 kOe for C875 is observed (Table 5). This lowering in field value suggests that the capability for the incorporation of Zr^{4+} decreases with increasing calcination temperature. Thus, Zr^{4+} ions would be progressively released from the hematite lattice, forming a novel population of zirconia particles, probably with a nanometric size.

An ILEEMS measurement at RT was performed for sample C925 (Fig. 11). The emission spectrum has the same shape and spectral components as does the transmission spectrum (Fig. 10), however with a significantly higher contribution of the α-Fe_2O_3, i.e., 75% instead of 52%. This finding is clear evidence that the hematite particles are at the surface of the zirconia grains. It should be mentioned that the hyperfine parameters for the α-Fe_2O_3 and for Fe^{3+} in the zirconia phase as obtained from the ILEEMS are within error limits identical to the values fitted to the transmission MS.

The above data show that the Fe^{3+} ions solubility in the stabilized $Zr_{0.9}Fe_{0.1}O_{1.95}$ solid solution starts to decrease at about 875 °C which results in the formation of possibly Zr^{4+}-substituted-hematite nanoparticles at the surface of the zirconia grains. The

Fig. 9. Mössbauer spectra collected at RT (left), 80 K (right) of powder ZF-7U calcined in air at 625, 850, and 875 °C.

Table 5

Mössbauer parameters at RT and 80 K for powder ZF-7U calcined in air at different temperatures. H_{hf}: hyperfine field; $2\varepsilon_Q$: quadrupole shift; ΔE_Q: quadrupole splitting; δ: isomer shift; and RA: relative spectral area.

| Calcination temperature (°C)	Hematite sextet				Fe^{3+} doublet		
	H_{hf} (kOe)	$2\varepsilon_Q$ (mm/s)	RA (%)	δ (mm/s)	ΔE_Q (mm/s)	RA (%)	δ (mm/s)
RT							
As-prepared	–	–	–	–	0.89	100	0.33
625	–	–	–	–	0.89	100	0.33
850	–	–	–	–	0.91	100	0.33
875	513	−0.19	9	0.38	0.94	91	0.34
925	514	−0.22	52	0.36	0.85	48	0.34
1025	515	−0.20	81	0.37	0.98	19	0.38
1225	516	−0.19	93	0.36	0.89	7	0.42
80 K							
As-prepared	–	–	–	–	0.89	100	0.46
625	–	–	–	–	0.89	100	0.46
850	–	–	–	–	0.91	100	0.45
875	532	−0.11	10	0.50	0.90	90	0.45
925	532	−0.21	52	0.47	0.90	48	0.46
1025	533	−0.21	81	0.47	0.83	19	0.49
1225	534	−0.09	93	0.47	0.85	7	0.50
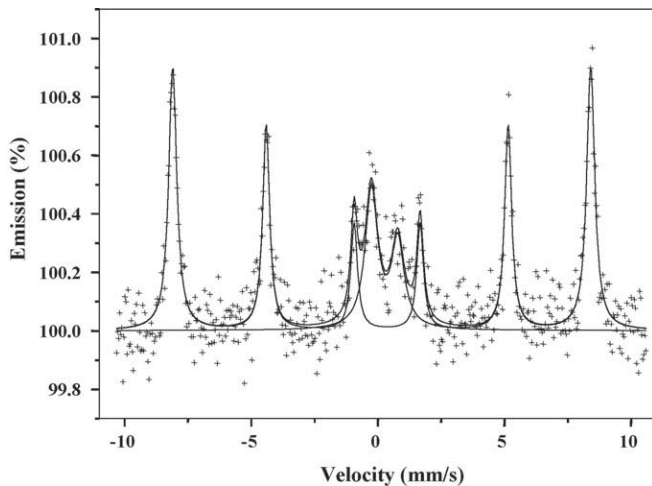
Fig. 11. ILEEMS spectrum of powder ZF-7U calcined in air at 925 °C collected at RT.

continuous decrease in the Fe^{3+} content in the stabilized phase upon the increase in calcination temperature causes the transformation into the monoclinic zirconia phase, which contains no appreciable amount of iron. The Zr^{4+} ions would be progressively released from the hematite phase, forming a novel population of monoclinic zirconia nanoparticles. Size effects do not appear to be directly connected to these changes.

4. Conclusions

The synthesis of Fe^{3+}-stabilized zirconia by the nitrate/urea combustion route was investigated. Using several characterization techniques, including XRD, FEG-SEM and notably Mössbauer spectroscopy, it was possible to determine the appropriate amount of urea (6–9 times the so-called stoichiometric proportion) that allows to obtain a totally stabilized Zr$_{0.9}$Fe$_{0.1}$O$_{1.95}$ solid solution without free iron oxide species. The zirconia solid solution is essentially tetragonal, but the presence of the cubic phase could not be ruled out. The crystallite size is below about 10 nm. An in-depth study of the thermal stability in air showed that the Fe^{3+} ions solubility in the stabilized Zr$_{0.9}$Fe$_{0.1}$O$_{1.95}$ solid solution starts to decrease at about 875 °C which results in the formation of possibly Zr^{4+}-substituted-hematite nanoparticles at the surface of the zirconia grains and further provokes the progressive transformation into the monoclinic zirconia phase.

References

[1] M. Yashima, T. Hirose, S. Katano, Y. Suzuki, M. Kakihana, M. Yoshimura, Phys. Rev. B 51 (1995) 8018.
[2] M.M.R. Boutz, A.J.A. Winnubst, F. Hartgers, A.J. Burgraaf, J. Mater. Sci. 29 (1994) 5374.
[3] S. Davison, R. Kershaw, K. Dwight, A. Wold, J. Solid State Chem. 3 (1988) 47.
[4] F.J. Berry, M.H. Loreto, M.R. Smith, J. Solid State Chem. 83 (1989) 91.
[5] F.J. Berry, S. Jobsen, M.R. Smith, Hyperfine Interact 46 (1989) 607.
[6] H.P. Beck, C. Kaliba, Mater. Res. Bull. 25 (1990) 1161.
[7] P. Li, I.-W. Chen, J.E. Penner-Hahn, J. Am. Ceram. Soc. 77 (1994) 118.
[8] I.B. Inwang, F. Chyad, I.J. Mc Colm, J. Mater. Chem. 5 (1995) 1209.
[9] S. Popović, B. Gržeta, S. Štefanić, I. Czakó-Nagy, S. Musić, J. Alloys Compds. 241 (1996) 10.
[10] G. Štefanić, S. Music, S. Popovic, J. Mol. Struct. 480–481 (1999) 627.
[11] G. Štefanić, B. Grzeta, S. Music, Mater. Chem. Phys. 65 (2000) 216.
[12] G. Štefanić, B. Grzeta, K. Nomura, R. Trojko, S. Music, J. Alloys Compds. 327 (2001) 151.
[13] V.V. Kriventsov, D.I. Kochubey, Yu.V. Maximov, I.P. Suzdalev, M.V. Tsodikov, J.A. Navio, M.C. Hidalgo, G. Colón, Nucl. Instr. Meth Phys. Res. 470 (2001) 341.
[14] J.A. Navio, M.C. Hidalgo, G. Colon, S.G. Botta, M.I. Litter, Langmuir 17 (2001) 202.
[15] K. Chen, L. Dong, Q. Yan, Y.J. Chen, Chem. Soc., Faraday Trans. 93 (1997) 2203.
[16] Y. Okamoto, T. Kubota, Y. Otho, S. Nasu, J. Phys. Chem. B 104 (2000) 8462.
[17] J.Z. Jiang, F.W. Poulsen, S. Mørup, J. Mater. Res. 14 (1999) 1343.
[18] P. Ghigna, G. Spinolo, U. Anselmi-Tamburini, F. Maglia, M. Dapiaggi, G. Spina, L. Cianchi, J. Am. Ceram. Soc. 121 (1999) 301.
[19] F. Maglia, U. Anselmi-Tamburini, G. Spinolo, A. Munir, J. Mat. Synth. Proc. 7 (1999) 327.
[20] A.E. Bohé, J.J.A. Gamboa, D.M. Pasquevich, Mater. Sci. Eng. A 273–275 (1999) 218.
[21] R.H.G. Kiminami, J. Mater. Sci. Lett. 9 (1990) 373.
[22] O. Quénard, Ch. Laurent, M. Brieu, A. Rousset, Nanostruct. Mater. 7 (1996) 497.
[23] O. Quénard, E. De Grave, Ch. Laurent, A. Rousset, J. Mater. Chem. 7 (1997) 2457.
[24] E. Flahaut, A. Govindaraj, A. Peigney, Ch. Laurent, A. Rousset, C.N.R. Rao, Chem. Phys. Lett. 300 (1999) 236.
[25] E. Flahaut, A. Peigney, Ch. Laurent, A. Rousset, J. Mater. Chem. 10 (2000) 249.
[26] P. Coquay, E. De Grave, A. Peigney, R.E. Vandenberghe, Ch. Laurent, J. Phys. Chem. B 106 (2002) 13186.
[27] P. Coquay, A. Peigney, E. De Grave, E. Flahaut, R.E. Vandenberghe, Ch. Laurent, J. Phys. Chem. B 109 (2005) 17813.
[28] A. Cordier, A. Peigney, E. De Grave, E. Flahaut, Ch. Laurent, J. Eur. Ceram. Soc. 26 (2006) 3099.
[29] A. Ringuede, J.A. Labrincha, J.R. Frade, Solid State Ionics 141–142 (2001) 549.
[30] V.G. de Resende, F.L. Garcia, A. Peigney, E. De Grave, Ch. Laurent, J. Alloys Compds 471 (2009) 204.
[31] K.C. Patil, Bull. Mater. Sci. 16 (1993) 533.
[32] S.R. Jain, K.C. Adiga, V.R. Pai Verneker, Combust. Flame 40 (1981) 71.

[33] Y. Zhang, G.C. Stangle, J. Mater. Res. 9 (1994 1997).
[34] J. Rodriguez-Carvajal, Abstracts of the Satellite Meeting on Powder Diffraction of the XV Congress of the IUCr, Bordeaux, 1990, p. 127.
[35] R.C. Garvie, P.S. Nicholson, J. Am. Ceram. Soc. 55 (1972) 303.
[36] I.C. Madsen, N.V. Scarlett, L.M.D. Cranswick, T. Lwin, J. Appl. Cryst. 34 (2002) 409.
[37] E. De Grave, R.E. Vandenberge, C. Dauwe, Hyperfine Interact 161 (2005) 147.
[38] G.M. da Costa, E. De Grave, L.H. Bowen, P.M.A. de Bakker, R.E. Vandenberghe, Clays Clay Minerals 43 (1995) 562.
[39] F. Legorreta Garcia, A. Peigney, Ch. Laurent, Mater. Res. Bull. 43 (2008) 3088.